D. Eckardt
DFVLR
Institut für Luftstrahlantriebe,
Porz-Wahn, West Germany

Instantaneous Measurements in the Jet-Wake Discharge Flow of a Centrifugal Compressor Impeller

One of the critical problems in centrifugal compressor design is the diffuser-impeller interaction. Up to now, theoretical models, which describe one of the salient features of this problem, the impeller discharge mixing process, appear to be proved experimentally only at low tip speeds. In the present study investigations on this subject were accomplished in the vaneless diffuser of a low-pressure ratio centrifugal compressor, running at tip speeds of 300 m/s. Detailed, instantaneous measurements in the impeller discharge mixing zone were performed by high-frequency measuring systems. Relative velocity distributions at the exit of impeller blade channels show pronounced jet/wake-patterns. The radial extension of flow distortions in the vaneless diffuser entry region, caused by rotating wakes, reached up to higher radius ratios than predicted by theoretical models.

Introduction

Up to now a great number of experimental investigations on centrifugal pumps, as well as on compressors, at relatively low speeds have already provided a qualitatively good survey of the flow in centrifugal impellers, here the publications of Acosta, et al. [1],[1] Fujie [2], Senoo, et al. [3], and Fowler [4] have to be mentioned. But the actual impeller flow in modern high-speed, high-pressure ratio compressors, which is strongly affected by three-dimensional boundary layers, secondary flows and flow separations is still beyond any theoretical prediction. Therefore further experimental investigations on highly-loaded impellers at realistic operating conditions have to be carried out.

One of the critical problems in the design of highly loaded centrifugal compressors is the interaction between the impeller and diffuser flow. For instance, in small gas turbines the diffuser vanes must be coupled very closely to the rotor, that means the blades are exposed immediately to the strongly distorted unsteady flow leaving the impeller.

In order to evaluate these flow phenomena and the accompanying mixing losses, Dean and Senoo [5], and later in simpler form, Johnston and Dean [6] introduced an analysis, based on a two-dimensional jet/wake model. As a result of their theoretical considerations, they could show that the unsteady unsymmetrical flow at the rotor outlet should be attenuated very rapidly and mixed out completely within a small radial distance downstream of the impeller. A detailed experimental examination of these theories—especially in the field of medium—and high-pressure ratio compressors— is not yet available.

Since 1970 the DFVLR-Institut für Luftstrahlantriebe has carried out a research program on a centrifugal compressor; its maximum pressure ratio, which will be obtained in the future, reaches $PR = 7$ at 27000 rpm. The purpose of this investigation is to improve the insight into the real flow phenomena in centrifugal compressors and especially into the mixing process just downstream of the impeller. This paper deals with measuring techniques, used in the aforementioned experimental work, and furthermore submits first test results.

Test Rig

The centrifugal compressor is driven by a dc-motor with a maximum power input of about 1500 kW. The motor speed can be continuously varied from zero to maximum, permitting—by means of a gear-box—an upper shaft speed limit of 27000 rpm. Current tests are run up to 18000 rpm and a pressure ratio $PR = 3.1$. An impeller tip diameter of 400 mm was selected in order to achieve flow channels, large enough compared with the dimensions of any measuring probes.

The centrifugal impeller, used in this investigation, is shown in Fig. 1 in a perspective view. This impeller, milled out of a block of aluminium alloy, has 20 radially ending blades. The main dimensions of the impeller are given in Fig. 2. The blade camber lines have ellipsoidal shapes in cylindric sections, as shown in the bottom sketch of Fig. 2. The tip clearance is changing during compressor operation, due to centrifugal forces and thermal expansion of materials at higher running temperatures. The gaps are varying between 0.8 mm at zero and 0.25 mm at current maximum speed.

[1] Numbers in brackets designate References at end of paper.

Contributed by the Gas Turbine Division and presented at the Gas Turbine Conference, Zurich, Switzerland, March 31–April 4, 1974, of THE AMERICAN SOCIETY OF MECHANICAL ENGINEERS. Manuscript received at ASME Headquarters, November 27, 1973. Paper No. 74-GT-90.

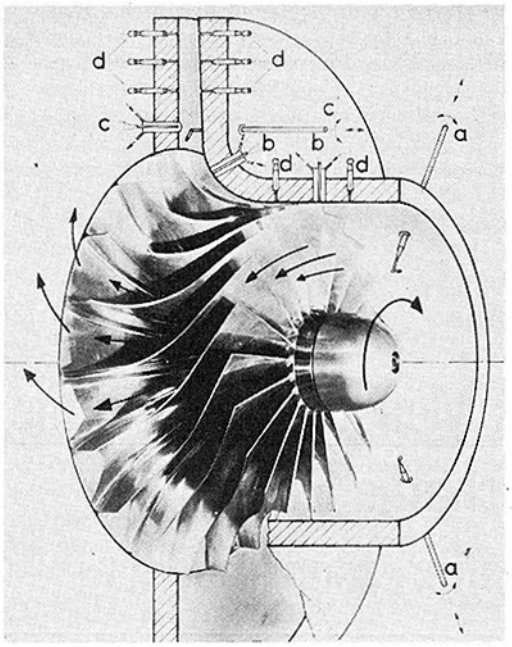

Fig. 1 View of centrifugal impeller and locations of various measurement systems: *(a)* Total pressure and temperature probes; *(b)* static pressure transducers; *(c)* total pressure transducer probes, flow angle hot-wire probes, time-avg total pressure probes; *(d)* time-avg static pressure adapters

The vaneless diffuser has a constant flow area to radius ratio $R/R_2 = 2$. Selection of a vaneless diffuser provides access to the impeller discharge region. The installation allows for vaned diffusers which will be tested in the future.

The diffuser is followed by a bend which turns the flow into an annular settling chamber of constant area.

The air leaves this chamber through a tangential discharge duct which contains a valve for throttling the flow.

Some preliminary tests showed that the tangential compressor outlet produced a severe distortion of the flow field with a strong nonsymmetry of flow parameters within the diffuser and even upstream of the rotor. In order to avoid these effects, an additional throttle ring was mounted near the outlet of the diffuser ($R/R_2 = 1.9$, Fig. 2). With this restriction the region of high mass flow on the compressor map, Fig. 3, to the right of the plotted choke line —was cut off. In the remaining compressor working region however, the distortion of the flow field was reduced to an insignificant level.

The test results submitted in this paper pertain to 3 compressor operating conditions, selected from the present test data and designated by $M1$, $M2$, and $M3$ on the compressor map (Fig. 3), as well as throughout this paper. Table 1 contains the complete data (shaft speed, mass flow, pressure ratio and efficiency) of these test points.

The schematic, cross-sectional view of the radial compressor in Fig. 1 illustrates also the mounting positions of the different measuring devices (all in the stationary system) used to obtain the results. Mainly measurements of the instantaneous static pressures along the casing within the rotor region and at the diffuser front and back walls were taken. Fluctuating total pressures and flow angles were determined over the exit-width b of a blade channel in 3 different radial locations downstream of the rotor, designated by $L1$, $L2$, and $L3$ and defined in Table 2.

Nomenclature

b = passage width in meridional plane
°C = deg Celsius
c = absolute velocity
c_p = specific heat at constant pressure
f = total pressure fluctuation coefficient $f = \sqrt{(\overline{P_i - P})^2_{\theta x}}/P_{\theta x} \cdot 100$ percent
K = deg Kelvin
$L1, L2, L3$ = measurement radial locations behind impeller exit (see Table 2)
$M1, M2, M3$ = test points (see compressor map Fig. 3 and Table 1)
m = coordinate along blade tip contour in meridional plane, beginning at inducer tip
$\dot{m}$ = mass flow rate
n = shaft speed
P = total pressure
PR = total pressure ratio
PS = pressure-side
p = static pressure
pr = static pressure ratio
R = radius
r = radial coordinate
SS = suction-side
s = length of blade tip contour in meridional plane (see Fig. 2)
T = total temperature
T_E = equivalent total temperature (definition in text)
TR = total temperature ratio $TR = (T_{3\theta x} - \bar{T}_4)/(\bar{T}_4 - \bar{T}_0) \cdot 100$ percent
t = static temperature
t = distance between impeller blades $t = 2\pi R/Z$
u = impeller (metal) velocity
w = relative velocity
x = axial coordinate
Z = number of blades
α = flow angle between absolute velocity vector and tangential direction in the sense of rotation
δ = pressure correction factor for standard conditions $\delta = P/1.01325$ bar
η = isentropic efficiency, total to total, measuring stations, see Fig. 2. Used definition:
η_{TT04} = $T_0[(P_4/P_0)^{(\kappa-1)/\kappa} - 1]/(T_4 - T_0)$
θ = temperature correction factor for standard conditions $\theta = T/288.1$ K
θ = tangential angular coordinate, positive in sense of rotation
κ = ratio of specific heats
μ = slip factor $\mu = c_{3\theta}/u_3$
ξ = relative total pressure loss-coefficient $\xi = (P_{\text{rel, 3, }\theta x} - P_{\text{rel, is, 3}})/P_{\text{rel, is, 3}} \cdot 100$ percent
ω = secondary flow coefficient $\omega = (w_{\theta\text{th}} - w_\theta)_{\theta x}/u_2 \cdot 100$ percent

Subscripts

0, 1, 2, 3, 4 = stations in the stage (see Fig. 2)
i = fluctuating signal value
j = jet
is = isentropic
r = component in radial coordinate
rel = relative coordinate system
TT = total to total
t = tip
w = wake
x = component in axial coordinate
θ = component in tangential coordinate

Superscripts

° = deg
− = time-averaged property
~ = mass-flow averaged property
→ = vector quantity

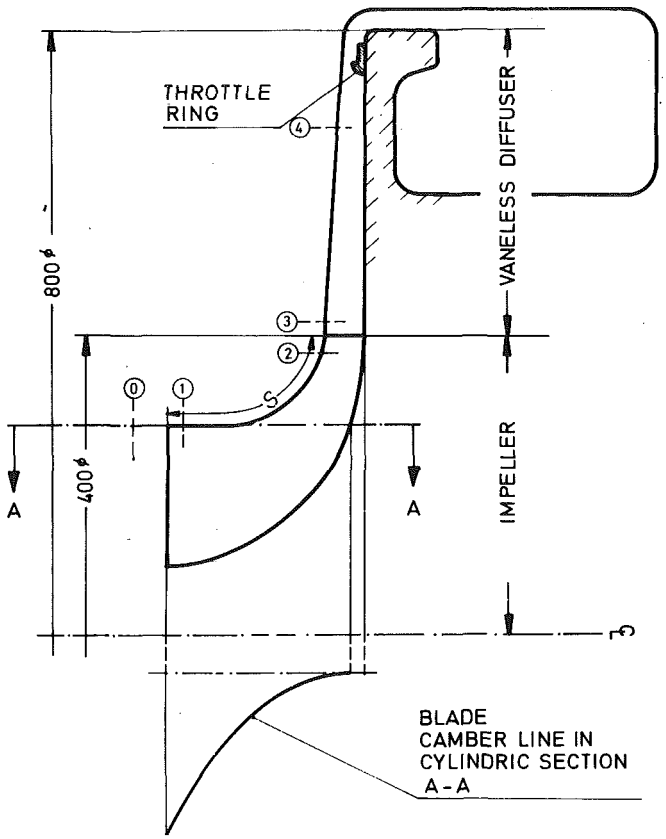

Fig. 2 Cross-sectional view of flow passages through centrifugal impeller and vaneless diffuser, with measurement location index. Dimensions in mm.

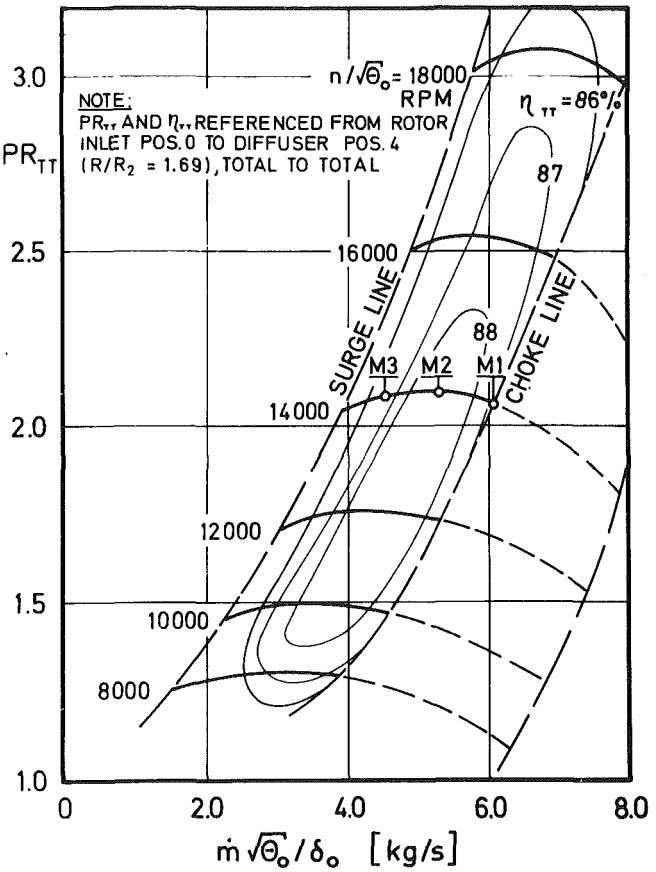

Fig. 3 Compressor map. Points of reported, detailed investigations are designated by *M*1, *M*2, and *M*3

Experimental Techniques

In order to perform quantitatively accurate measurements of the main flow parameters in highly loaded centrifugal compressors, adequate high-frequency measuring techniques are necessary. For example, the grossly turbulent discharge flow in the mixing zone is composed of strong velocity and flow angle fluctuations which is further complicated by unsteady flow behavior in the relative system—e.g., by transient unstable flow separations. The strong pressure pulsations resulting from this flow pattern and the high running temperatures, increase the demand on the measuring equipment. In the present investigation, which is especially aimed at the analysis of the flow processes in the mixing zone, mainly measuring systems of high natural frequency were considered.

At a shaft speed of 18000 rpm—corresponding to a blade passing frequency of 6 kHz—they must be able to indicate flow parameters, fluctuating at frequencies considerably higher than the blade frequency, e.g., at the transition from blade pressure to suction side, where the flow parameters may be rapidly changing. The natural frequency of the measuring systems had to be at least 100 kHz, and the accuracy should be high and stable over a long time.

Several years ago DFVLR—Institut für Luftstrahlantriebe started a research program concentrated on the development of new measuring techniques, well-suited for experimental work in turbomachines. This program is continuing.

Hot-wire anemometry, often applied to low-loaded radial compressors, was also considered for quantitative velocity measurements in highly-loaded compressors. But in addition to the questionable hot-wire durability, the flow at centrifugal impeller discharge is so complicated, because of fluctuations in velocities, densities, directions and turbulence intensities, that at the moment it seems very difficult to separate the different parameters affecting the hot-wire heat transfer.

A contactless Laser-velocimeter is currently under laboratory tests. It should allow measurement of two-dimensional flow velocity components up to about 400 m/s at an accuracy of nearly ±1 percent and ± 1 deg in flow direction.

The test results submitted in this paper rely essentially on the experimental techniques, described in the following section.

Table 1 Compressor characteristics in the test points

Test point	$n/\sqrt{\theta_0}$ [rpm]	$\dot{m}\sqrt{\theta_0}/\delta_0$ [kg/s]	PR_{TT04} [−]	η_{TT04} [percent]
*M*1	14000	6.09	2.061	86.8
*M*2	14000	5.31	2.094	88.0
*M*3	14000	4.53	2.086	86.5

Table 2 Measurement location behind impeller exit

Meas. radial location	R/R_2 [−]	$R-R_2$ [mm]
*L*1	1.017	3.4
*L*2	1.039	7.7
*L*3	1.089	17.7

Measurements of Oscillating Pressures

The unsteady wall pressures along the impeller outer contour and at the front- and back-walls of the diffuser entry region were recorded by means of pressure transducers, mounted in the compressor casing.

The sketch on the left hand side of Fig. 4 presents the transducer mounting. These are miniature pick-ups on semiconductor basis with a natural frequency of about 120 kHz and a compensated temperature range up to 80 deg C. In order to reduce the thermal zero shift and to extend the working temperature range

the transducers were installed in special cooling jackets.

As an example of these measurements Fig. 5 shows oscilloscope traces of the fluctuating wall pressures at 4 different shroud positions. The ratio m/s means the dimensionless coordinate along the impeller outer contour, starting at inducer tip, as indicated in Fig. 2.

To take measurements of the fluctuating total pressures immediately downstream of the impeller, special probes were designed and manufactured, which were equipped also by semiconductor pickups. The drawing on the right-hand side of Fig. 4 demonstrates the main dimensions of these probes, which are suitable for measurements in the mixing zone, due to their flow angle insensitivity of ±25 deg. The natural frequency of the probe-installed transducers, reaches up to 100 kHz, whereas the pressure range is temperature compensated up to 165 deg C. Immediately behind the transducer steel diaphragm a temperature sensor (thermistor) is installed by means of which the average diaphragm temperature can be determined as an additional parameter. The semiconductor pickups used for static and total pressure measurements were investigated in detail under laboratory conditions. During calibration tests with a special pressure generator, which is described in [7], trapezoidal pressure fluctuations with a frequency up to 5.5 kHz and with amplitudes of about 1 bar were supplied to the transducers. From this it was concluded that the selected pickups should be suited to transmit the pressure fluctuations expected in the centrifugal compressor.

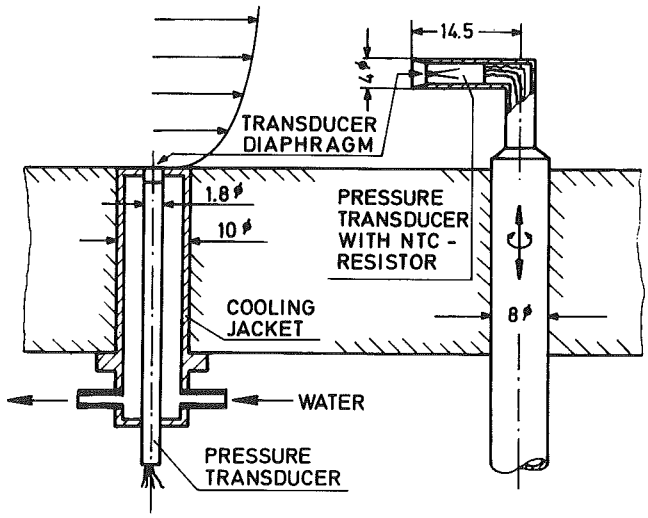

Fig. 4 Mounting of static pressure transducers and total pressure transducer probes. Dimensions in mm.

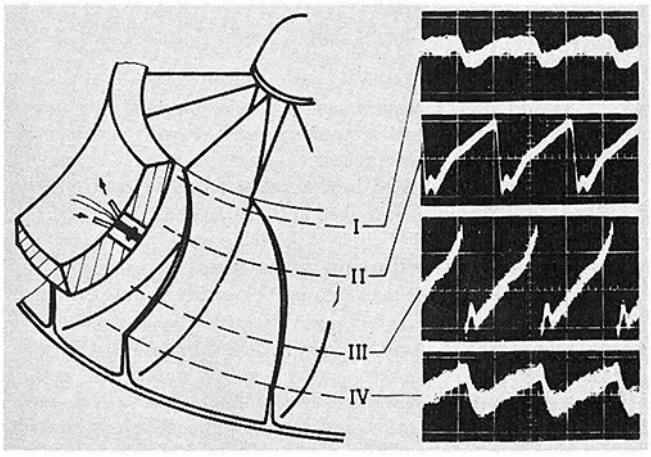

Fig. 5 Wall pressure traces along the impeller shroud. Test point *M*1 (I, II, III, IV: m/s = 0.059, 0.434, 0.868, 1.000).

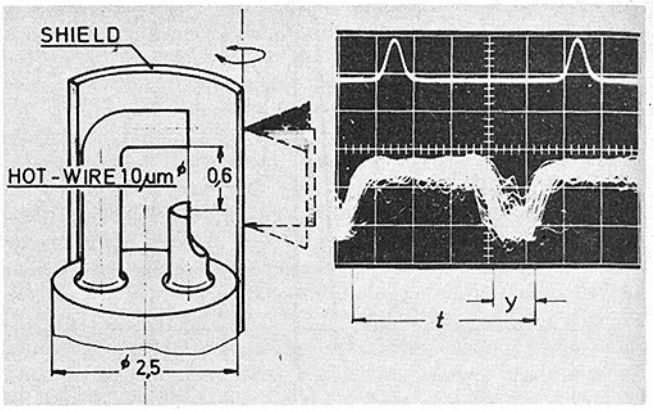

Fig. 6 Instantaneous flow-direction measurement technique. Left: head of hot-wire probe, right upper trace: reference signal of exit tip clearance transducer, right lower trace: typical hot-wire probe signal (~50 times), t = 1 blade period, y = hot-wire in the wake of shield.

Laboratory tests on the effect of ambient temperature on the transducer behavior showed that their sensitivity remains nearly unaffected by temperature changes, whereas the thermal zero shift cannot be predicted for each case. That means that the transducers measure unsteady pressure variation with sufficient accuracy, but not the pressure level. Therefore, in the compressor tests the true time-weighted pressures were determined by means of special techniques, described in the next section. A detailed description of these methods is given in [7].

Measurement of Time-Weighted Pressures

It is well-known that in strongly fluctuating flows the mean pressures, indicated by pneumatic systems—consisting for example of a wall orifice, a connecting line and an inert instrument—differ more or less from the real time-averaged values. The magnitude of possible errors depends essentially on the shape of measuring orifice and on the amplitude and form of the fluctuating pressures. However, using a special pneumatic probe [7], the indicated mean pressure can be reduced to the time-weighted value by means of a correlation method, provided that the dynamic part of the oscillating pressure at the same measuring point is known. This method was used in order to determine the oscillating absolute wall pressures at the compressor casing in the rotor region. This was performed by superposing the pressure oscillation, indicated by the above mentioned transducers, to the correlated mean pressure.

For determining the time-weighted total pressures in the different radial locations $L1$, $L2$, $L3$ (Table 2) downstream of the impeller, special pitot-probes were used, the head of which consists of a capillary tube connected to a standard pressure transducer [7]. This measuring system is completely filled with oil and indicates directly the true time-averaged pressures.

Some experimental results are shown in Fig. 7 and 8. Fig. 7 contains a plot of the measured wall pressure distributions for the 3 test points $M1$, $M2$, and $M3$ (Table 1, Fig. 3). The results are given as lines of constant static pressure ratio p/p_0. For the test point $M1$ Fig. 8 presents the total pressure distribution, determined in the stationary system at $L1$. The graph shows the contours of one impeller exit channel. The twisted blade wakes were found by the use of a new technique for instantaneous flow angle measurements. This method is described next.

Measurement of Instantaneous Flow Directions

The basic details of the probe, developed for the measurement of instantaneous flow directions, is shown on Fig. 6. The probe is operated by a conventional DISA-55 D 00 anemometer. For measurements at the exit of a centrifugal impeller the probe is mounted in such a position, that the hot-wire is parallel to the axis of impeller rotation (x axis). A 120 deg annular segment, the leading edge of which is sharpened, is mounted at the head of the

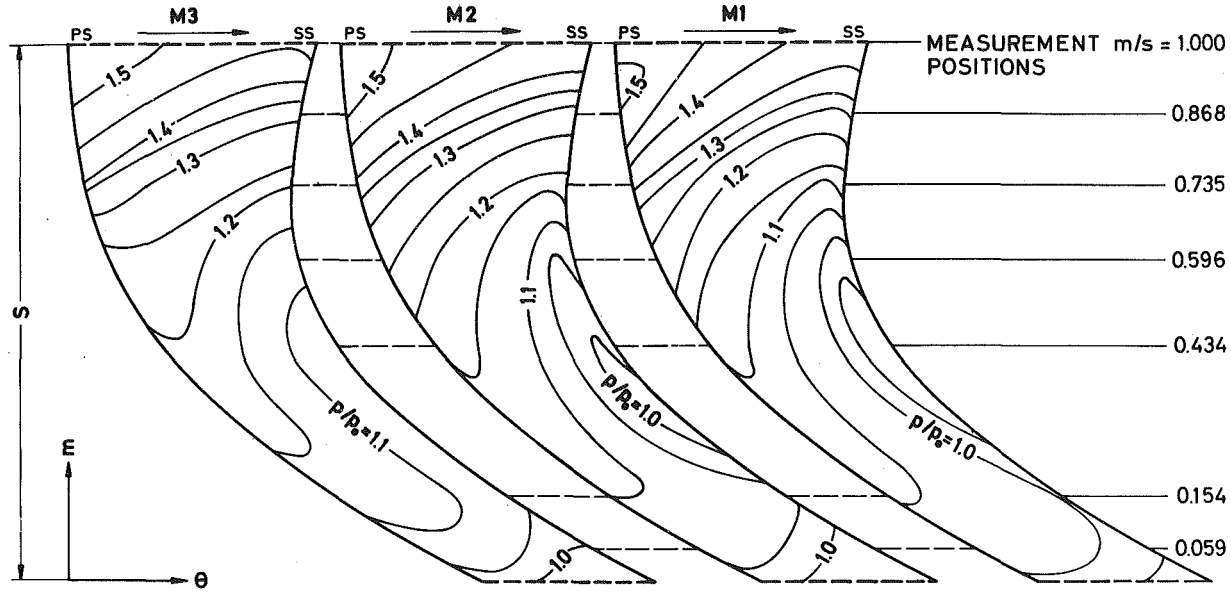

Fig. 7 Wall pressure distribution of one blade channel along the compressor shroud at test points *M*1, *M*2, and *M*3 (lines of constant static pressure ratio)

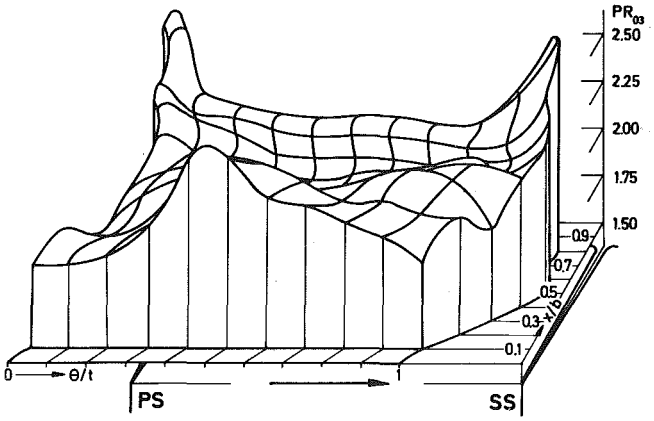

Fig. 8 Total pressure distribution at the exit of one blade channel. Test point *M*1, measurement location *L*1.

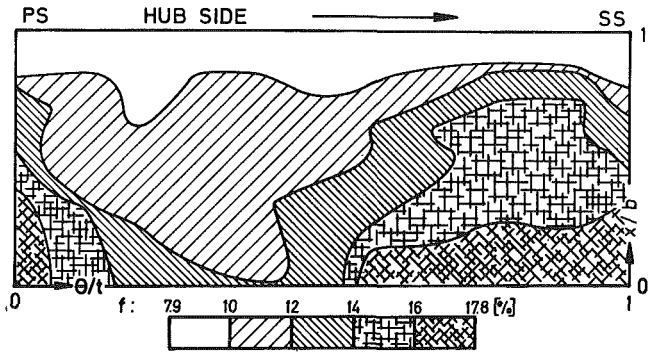

Fig. 9 Distribution of total pressure fluctuation coefficient *f* at the exit of one blade channel. Test point *M*1, measurement location *L*1.

probe as a shield. The purpose of the probe is to measure the time-dependent flow angle α between the absolute velocity vector and the tangential direction θ in the centrifugal impeller discharge flow. In the jet/wake-pattern there is an instantaneous change in flow direction between the blades. The probe measuring angle is defined as the angle between the imaginary connection line of shield leading edge to hot-wire and the tangential direction θ. The lower trace on the right-hand side of Fig. 6 shows a typical probe signal, which is periodic with t.

As the rotating wake passes the probe at small flow angles α, the hot-wire lies in direct flow impingement. This causes a high signal voltage during the time t-y. When the jet arrives, the flow to the wire is screened. The wire lies in the wake of the shield and shows a small output voltage during the time y. At the transition point from high to low signal voltage the flow has the same angle as the adjusted probe measuring angle. By measuring the time ratio y/t on the oscilloscope trace, it is possible to find the location between two blades, where the adjusted probe angle exists. By relating the hot-wire signal to a tip clearance signal, shown on right-hand side of Fig. 6, upper trace, one receives the position of the blade wakes relative to the real blade tips at the impeller exit. By varying the measuring angle and traversing the probe over the diffuser width at various radial locations Fig. 10 results for the distribution of absolute velocity directions relative to one impeller exit channel.

The described measurement technique is based on the high time-resolution power of hot-wire anemometry. There is no need for signal amplitude interpretation; only the various time periods are measured.

During extensive laboratory tests the frequency characteristics of the measuring system were recorded with the deduction, that in the investigated speed range there are already small deviations in signal phase-angles, which have to be considered in data interpretation.

Logging and Reduction of Unsteady Data

The oscilloscope traces of Fig. 5 and Fig. 6 illustrate the unsteady character of flow. These records originate from the superposition of 50–100 single traces, the intensity of exposure yields the impression of the statistically mean signal trace. One single trace may deviate—for instance by a shift in the separation point in the relative system—significantly from the average trace. On the premises of constant shaft speed the measurement signals are exactly periodical and then the averaging of fluctuating signals to statistically mean unsteady signal-traces by means of electronics is possible. In this way random signals are extinguished. With an electronic set on the basis of the so-called Synchronized Sampling Technique (SST), the basic principle of which we will not explain here, it is possible to clean highly turbulent or buried-in-noise sig-

nals of pressure transducers or hot-wire direction probes of irregularly distributed disturbances and to get a delayed, retarded output of these high-frequency signals. This enables further processing of these signals in digital form. For instance it is possible to resolve a signal trace over one blade spacing, as shown in Fig. 5, in 300 digital values, to store them on tape and to do the further processing, data reduction, plotting, etc., under digital computer control.

Experimental Results and Discussion

The following selection of unsteady test data outline the general possibilities of the present measurement techniques for typical examples of centrifugal impeller discharge flow.

As an example of the results of unsteady static pressure measurements along the shroud of the centrifugal impeller, Fig. 7 shows the wall-pressure distribution for one blade channel at the measuring points $M1$, $M2$, and $M3$ in the compressor map (Fig. 3), drawn as lines of constant static pressure ratio. Most striking at the higher mass flows are the areas of low static pressures at the suction side in the region of radial turning and the bending of the lines to circumferential direction near the channel exit at the suction side. It may be presumed, that there will be a chance for

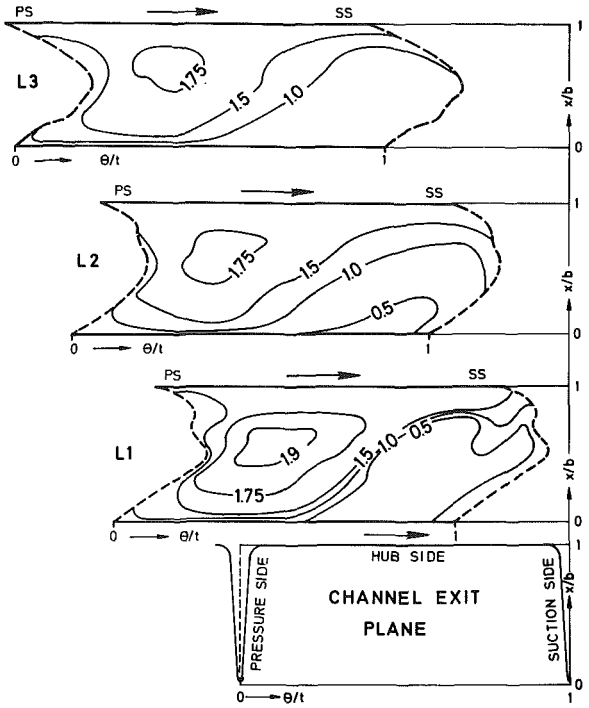

Fig. 10 Distribution of constant flow angle ratio α/α_{DESIGN}, relative to the exit of one blade channel. Test point $M1$, radial measurement locations $L1$, $L2$, and $L3$.

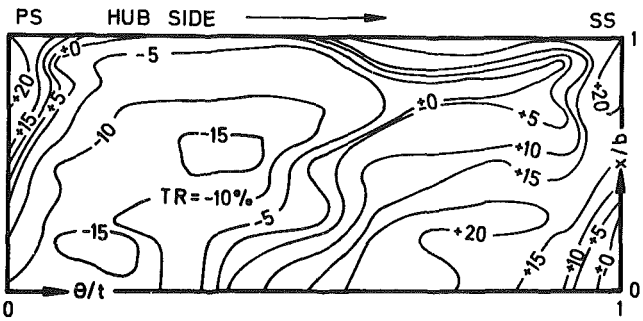

Fig. 11 Distribution of total temperature ratio TR at the exit of one blade channel. Test point $M1$, measurement location $L1$.

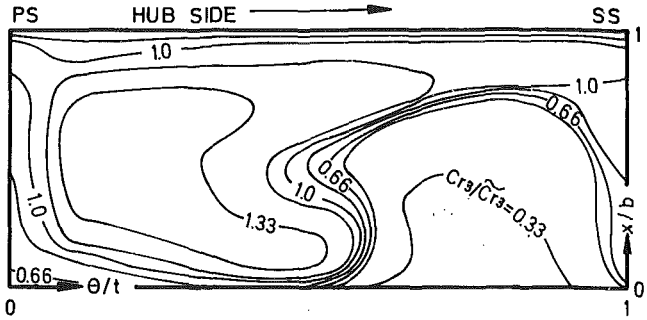

Fig. 12 Distribution of local radial velocity component c_{r3}, related to mass-mean value, at the exit of one blade channel. Test point $M1$, measurement location $L1$.

prediction of the location of separation point, dependent on shaft speed and mass flow, by these wall-pressure maps.

Fig. 8 presents the distribution of local total pressures $P_{3\theta x}$ related to the total pressure P_0 at compressor inlet for test point $M1$. The limitation lines of one blade spacing are a result of the unsteady direction measurements (Fig. 10). The most striking point of this total pressure distribution is the salient pressure peaks near the hub, which are possibly caused by the pronounced blade wakes in this area. One possible output of previously mentioned Synchronized Sampling Technique (SST) is the rms-value of signal oscillations. E.g., Fig. 9 shows the local total pressure fluctuation for the pressure distribution of Fig. 8. Fluctuation coefficient f is defined as

$$f = \sqrt{\overline{(P_i - P)^2_{\theta x}}} \,/\, P_{\theta x} \cdot 100 \text{ [percent]} \qquad (1)$$

The high total pressure fluctuation in the region of blade suction-side/shroud-side, with f reaching up to 17.8 percent, underlines the necessity for a measurement system like SST to get clear signal interpretation. By means of the presented flow direction measuring technique, Fig. 6, the distributions of constant flow angles were found and plotted for the test point $M1$ and 3 radial measuring locations $L1$, $L2$, and $L3$ in Fig. 10. The flow direction mapping is bounded by the time-mean position of (dashed-drawn) blade wakes, which are skewed by friction at the diffuser walls and displaced with respect to the impeller channel exit. Most striking are the high angle-differences of more than 30 deg. in level $L1$ with a steep direction gradient near the suction-side/shroud-side corner. With increasing radial distance from the impeller the direction distribution is smoother; at location $L3$ the difference is less than 20 deg and changes continuously, ($\alpha_{DESIGN} \approx 20$ deg).

The application of the previously described measurement techniques yields by direct measurements over a certain level behind the impeller: 1 the total pressure distribution in absolute system, 2 the distribution of absolute flow directions and 3 the static pressure distribution, which is found by linear interpolation between the measurements at diffuser front- and back-walls.

By measurements with a conventional stagnation temperature probe at $R/R_2 = 1.69$ outside the mixing zone, we calculated the mass-mean total temperature $\tilde{T}_4$. From this temperature and results of measurements directly behind the impeller, we determined by means of the enthalpy rise—calculated by the Euler equation—iteratively the local velocity- and temperature-distributions in the investigated measuring plane.

As an example for the so determined temperature distributions Fig. 11 shows the results for test point $M1$ and measuring location $L1$. The plotted total temperature ratio TR is defined as

$$TR = (T_{3\,\theta x} - \tilde{T}_4) \,/\, (\tilde{T}_4 - \tilde{T}_0) \cdot 100 \text{ [percent]} \qquad (2)$$

For the illustrated test point: $\tilde{T}_4 - \tilde{T}_0 = 74$ centigrades. Local velocity triangles were obtained from the interpolation of 11 × 9 points for location $L1$ and 11 × 5 points for the location $L2$ and $L3$ over one blade spacing.

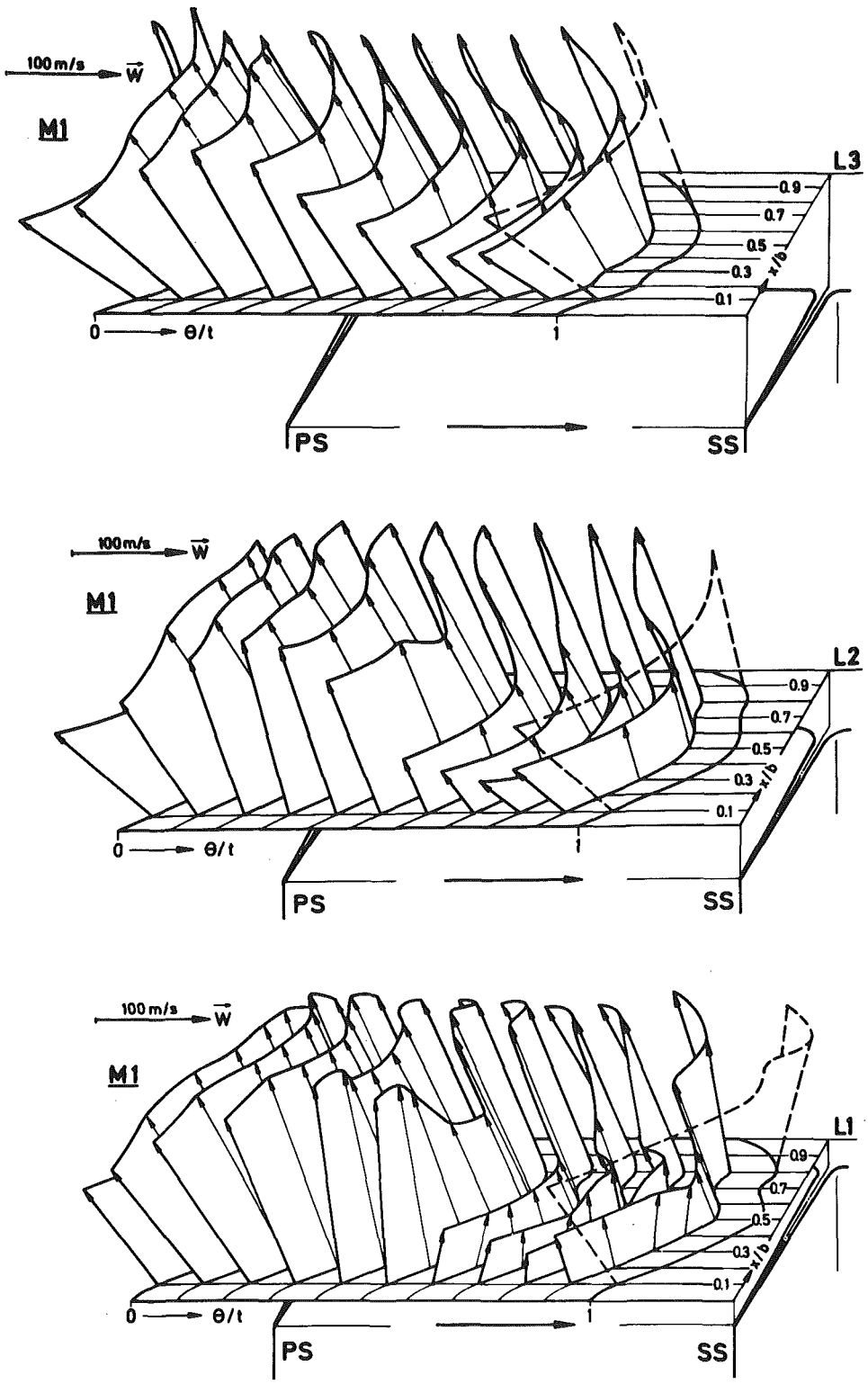

Fig. 13 Distributions of relative velocity vectors $\vec{w}$ at the exit of one blade channel. Test point $M1$, radial measurement locations $L1$, $L2$, and $L3$.

Fig. 12 shows the distribution of lines of constant radial velocity component c_{3r} for test point $M1$ at location $L1$, plotted on a rectangular channel frame. This figure and other interpreted tests show, that the ratio of mass flow in the wake to the total is about $\dot{m}_w/\dot{m} \approx 15$–$25$ [percent], this confirms the value stated in [8].

For an evaluation of the accuracy of the measurement techniques, mass balances were calculated for the test point $M1$ and the test results at locations $L1$, $L2$, and $L3$. The coincidence with the mass flow, measured by venturi nozzle, was for every point checked better than 1 percent. Possible reasons for this good agreement are—uniform axisymmetric flow conditions at test point $M1$, Fig. 3, due to the effect of the throttle ring, Fig. 2, and the compensation of possible local measurement uncertainties by the mass flow integration over 10×5 elements.

An impression of the complex flow structure at the exit of a highly-loaded centrifugal impeller is given by the distributions of

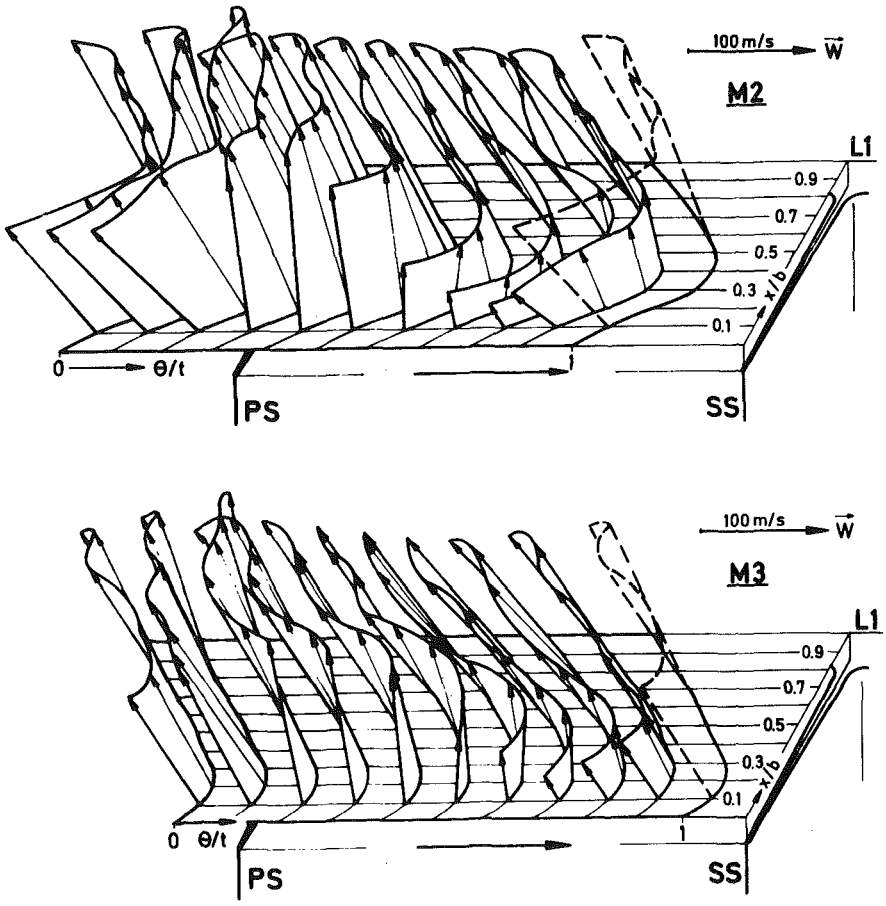

Fig. 14 Distributions of relative velocity vectors $\vec{w}$ at the exit of one blade channel. Test points *M*2 and *M*3, measurement location *L*1.

relative velocity vectors in 3 measuring locations $L1$, $L2$ and $L3$ at test point $M1$, shown in Fig. 13. Comparing the results of the 3 locations, fast mixing of velocity differences and the stabilization of velocity pattern between the wake region near the blade suction-side and diffuser front wall and the jet region in the diagonally opposite corner of the blade spacing is most evident. At measurement location $L3$ ($R/R_2 = 1.089$) axisymmetric homogenous flow is not yet achieved. The change of relative velocity pattern at the exit of a blade channel for reduced mass flows is shown in Fig. 14 with mass flows $M2$ and $M3$ in location $L1$. After knowing the results of Fig. 13 and 14 it was rather intriguing to evaluate the influence of secondary flow on this pattern—at least qualitatively. On the basis of a theoretical slip-factor, according to Stanitz' ($\mu = 0.89$) and the local radial absolute velocity component $c_{3r\,\theta x}$, a theoretical relative velocity component in tangential direction $w_{\theta \mathrm{th}}$ was calculated. The slip factor μ was taken as constant over the whole blade spacing of location $L1$. The latter assumption is incorrect, as Stanitz' later work showed, but for the sake of a short evaluation this simple proceeding should be sufficient. With the measured local w_θ-component, the theoretical $w_{\theta \mathrm{th}}$-value and the tip speed at impeller discharge a secondary flow coefficient ω was defined:

$$\omega = (w_{\theta th} - w_\theta)_{\theta x} / u_2 \cdot 100\ [\text{ percent }] \qquad (3)$$

w_θ is positive opposite to the sense of rotation. Fig. 15 shows the results of this evaluation for the test points $M1$ and $M3$, both plotted for measurement location $L1$. A view on these graphs shows, in the channel hub-side region where one would expect a tendency for cross flow from the pressure- to the suction-side, based on the pressure gradient, a marked tangential flow against direction of impeller rotation. Lennemann and Howard [9] report comparable results in this area for an unshrouded low-speed impeller; our

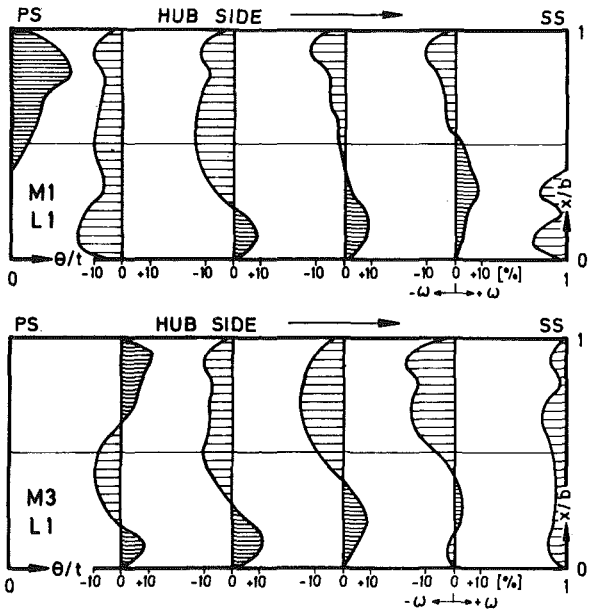

Fig. 15 Distributions of secondary flow coefficient ω at the exit of one blade channel. Test points *M*1 and *M*3, measurement location *L*1.

first results seem to confirm their general secondary flow pattern.

After consideration of relative velocity distributions at various mass flows and measurement locations behind the impeller exit we will now deal with the loss distribution resulting from measurements at the exit of a blade channel. As an example Fig. 16

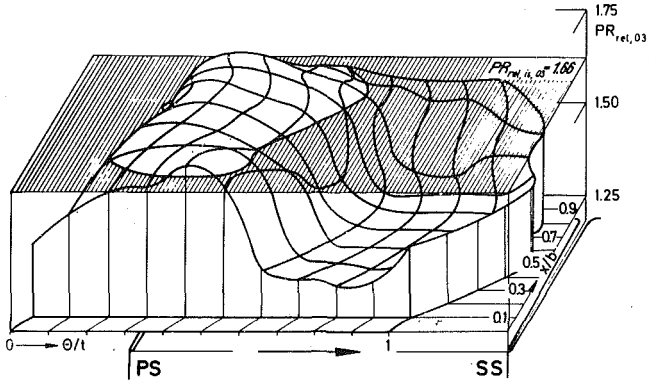

Fig. 16 Distribution of relative total pressure ratio $PR_{rel,03}$ compared to isentropic $PR_{rel,is,03}$-plane at the exit of one blade channel. Test point $M1$, measurement location $L1$.

shows the distribution of relative total pressure $P_{rel,3,\theta x}$, related to the total pressure at compressor inlet P_0, at measurement location $L1$ for test point $M1$. In this graph, a marked total pressure deficit governs the wake region near the suction-side/shroud-side corner. This figure and Fig. 9, 11, 12, and 13 yield a good prediction of the flow conditions in the wake. As a reference level to the measured relative total pressure distribution the isentropic relative total pressure rise was calculated for a stream tube, which starts at the blade tip at impeller inlet. From the so-called equivalent total temperature of rotor flow

$$T_E = t_1 + \frac{w_{1t}^2}{2\,c_p} + \frac{u_3^2 - u_{1t}^2}{2\,c_p} \qquad (4)$$

follows the relative isentropic total pressure ratio

$$PR_{rel,\,is,03} = P_{rel,\,is,\,3} \,/\, P_0 = (T_E/T_0)^{\kappa/(\kappa-1)} \quad , \qquad (5)$$

which is shown in Fig. 16 as the hatched plane.

The lowest losses are in the pressure hill of the jet area near the blade pressure-side. Dean [8] presumes, as a result of his data interpretation, an isentropic core in this region.

Fig. 17 shows the same data in a quantitatively clear form. By means of the calculated isentropic relative total pressure $P_{rel,is,3}$ for the shroud stream tube, lines of constant loss coefficient, defined as

$$\xi = (P_{rel,\,3,\,\Theta x} - P_{rel,\,is,3}) \,/\, P_{rel,\,is,3} \cdot 100\ [\text{percent}] \qquad (6)$$

are plotted over a blade channel exit in measuring level $L1$ for test point $M1$.

Conclusions

1 By means of presented unsteady measurement techniques a detailed, quantitative analysis of flow conditions behind a highly-loaded centrifugal impeller is possible.

2 The measurement of unsteady wall pressure distributions at the compressor casing along the impeller tip-contour renders quantitative statements on the blade loading and the beginning and extension of possible separation zones depending on compressor test point.

3 The relative velocity distributions measured directly behind the impeller, were characterized by a clearly limited region near the flow channel suction-side/shroud-side corner with low mass flow, high turbulences and losses, and a region with high c_r-component near the pressure side, with relatively stable flow and low total pressure losses. The location of a possible isentropic jet core could be determined approximately, but its existence has not been proved definitively as yet. The known jet/wake flow model was confirmed in principle. By further test interpretation it should be possible to come to at least empirical predictions of its three-dimensional distributions.

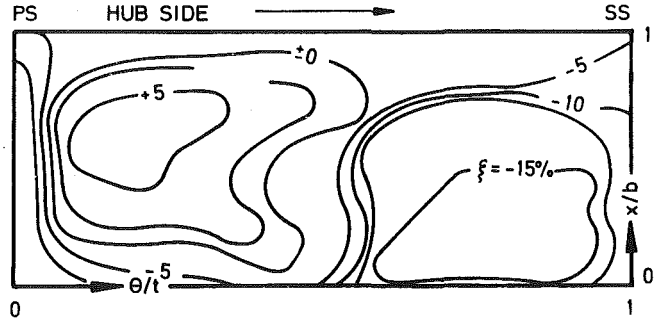

Fig. 17 Distribution of relative total pressure loss-coefficient ξ at the exit of one blade channel. Test point $M1$, measurement location $L1$.

4 Comparison of interpreted test results with calculated mixed state radius ratio according to the two-dimensional sudden expansion model [6] showed, that the flow was not yet axisymmetric at predicted $R/R_2 \approx 1.05$. Dean [8] mentions as probable reasons for this, a disturbance of velocity distributions also in meridional plane (and not only in θ-r plane) and $\dot{m}_w/\dot{m} \neq 0$, both conditions appeared in the test results.

5 Detailed secondary flow analysis at centrifugal impeller discharge seems to be possible with the presented measurement techniques. First approximated test interpretations tend to confirm the main points of the secondary flow pattern—presented in [9] for low-speed, unshrouded impellers—also for high-speed, high-pressure ratio centrifugals.

Acknowledgments

The work described in this paper was carried out as part of a research program on centrifugal compressors jointly sponsored by Forschungsvereinigung Verbrennungskraftmaschinen and Deutsche Forschungs- und Versuchsanstalt für Luft- und Raumfahrt.

References

1 Acosta, A. J., and Bowerman, R. D., "An Experimental Study of Centrifugal-Pump Impellers," TRANS. ASME, Nov. 1957, pp. 1821–1839.

2 Fujie, K., "Three-Dimensional Investigation of Flow in Centrifugal Impeller With Straight-Radial Blades," *Bulletin of JSME,* Vol. 1, 1958, No. 1, pp. 42–49.

3 Senoo, Y., Yamaguchi, M., and Nishi, M., "A Photographic Study of the Three-Dimensional Flow in a Radial Compressor," JOURNAL OF ENGINEERING FOR POWER, TRANS. ASME, July 1968, pp. 237–244.

4 Fowler, H. S., "Research on the Internal Aerodynamics of the Centrifugal Compressor," 11th Anglo-American Aeronautical Conference, London Sept. 8–12, 1969, Paper No. 19.

5 Dean, R. C., Jr., and Senoo, Y., "Rotating Wakes in Vaneless Diffusers," JOURNAL OF BASIC ENGINEERING, TRANS. ASME, Sept. 1960, pp. 563–570.

6 Johnston, J. P., and Dean, R. C., Jr., "Losses in Vaneless Diffusers on Centrifugal Compressors and Pumps," JOURNAL OF ENGINEERING FOR POWER, TRANS. ASME, Vol. 88, No. 1, Jan. 1966.

7 Weyer, H., and Schodl, R., "Development and Testing of Techniques for Oscillating Pressure Measurements Especially Suitable for Experimental Work in Turbomachinery," J. OF BASIC ENGINEERING, TRANS. ASME, Vol. 93, No. 4, December 1971, pp. 603–609.

8 Dean, R. C., Jr., "Notes on Advanced Radial Compressors," von-Karman-Institute for Fluid Dynamics, Lecture Series 50, May 15–19, 1972.

9 Lennemann, E., and Howard, J. H. G., "Unsteady Flow Phenomena in Rotating Centrifugal Impeller Passages," JOURNAL OF ENGINEERING FOR POWER, TRANS. ASME, Jan. 1970, pp. 65–72.